The Dual Function of the Mycobacterium tuberculosis FadD32 Required for Mycolic Acid Biosynthesis

Mathieu Léger, Sabine Gavalda, Valérie Guillet, Benoît van Der Rest, Nawel Slama, Henri Montrozier, Lionel Mourey, Annaïk Quémard, Mamadou Daffé, Hedia Marrakchi

▶ **To cite this version:**

Mathieu Léger, Sabine Gavalda, Valérie Guillet, Benoît van Der Rest, Nawel Slama, et al.. The Dual Function of the Mycobacterium tuberculosis FadD32 Required for Mycolic Acid Biosynthesis. Chemistry and Biology, 2009, 16, pp.510 - 519. 10.1016/j.chembiol.2009.03.012 . hal-03003389

HAL Id: hal-03003389
https://hal.science/hal-03003389

Submitted on 20 Nov 2020

HAL is a multi-disciplinary open access archive for the deposit and dissemination of scientific research documents, whether they are published or not. The documents may come from teaching and research institutions in France or abroad, or from public or private research centers.

L'archive ouverte pluridisciplinaire **HAL**, est destinée au dépôt et à la diffusion de documents scientifiques de niveau recherche, publiés ou non, émanant des établissements d'enseignement et de recherche français ou étrangers, des laboratoires publics ou privés.

Chemistry & Biology
Article

The Dual Function of the *Mycobacterium tuberculosis* FadD32 Required for Mycolic Acid Biosynthesis

Mathieu Léger,[1,2] Sabine Gavalda,[1,2] Valérie Guillet,[1,2] Benoît van der Rest,[1,2,3] Nawel Slama,[1,2] Henri Montrozier,[1,2] Lionel Mourey,[1,2] Annaïk Quémard,[1,2] Mamadou Daffé,[1,2,*] and Hedia Marrakchi[1,2,*]
[1]Centre National de la Recherche Scientifique (CNRS), Institut de Pharmacologie et de Biologie Structurale (IPBS), Département Mécanismes Moléculaires des Infections Mycobactériennes, 205 route de Narbonne, F-31077 Toulouse, France
[2]Université de Toulouse, Université Paul Sabatier (Toulouse III), IPBS, F-31077 Toulouse, France
[3]Present address: École Nationale Supérieure Agronomique de Toulouse, Avenue de l'Agrobiopole, BP 32607, Auzeville-Tolosane – F-31326 Castanet-Tolosan, Cedex
*Correspondence: mamadou.daffe@ipbs.fr (M.D.), Hedia.marrakchi@ipbs.fr (H.M.)
DOI 10.1016/j.chembiol.2009.03.012

SUMMARY

Mycolic acids are major and specific lipids of *Mycobacterium tuberculosis* cell envelope. Their synthesis requires the condensation by Pks13 of a C_{22}-C_{26} fatty acid with the C_{50}-C_{60} meromycolic acid activated by FadD32, a fatty acyl-AMP ligase essential for mycobacterial growth. A combination of biochemical and enzymatic approaches demonstrated that FadD32 exhibits substrate specificity for relatively long-chain fatty acids. More importantly, FadD32 catalyzes the transfer of the synthesized acyl-adenylate onto specific thioester acceptors, thus revealing the protein acyl-ACP ligase function. Therefore, FadD32 might be the prototype of a group of *M. tuberculosis* polyketide-synthase-associated adenylation enzymes possessing such activity. A substrate analog of FadD32 inhibited not only the enzyme activity but also mycolic acid synthesis and mycobacterial growth, opening an avenue for the development of novel antimycobacterial agents.

INTRODUCTION

One decade after the publication of the *Mycobacterium tuberculosis* genome sequence, impressive progress has been achieved toward the discovery and the understanding of specific and essential mycobacterial metabolic pathways. Among these is the lipid metabolism of the tubercle bacillus to which a high number of genes are dedicated. These lipids include mycolic acids, very long-chain (up to C_{90}) fatty acids (α-branched, β-hydroxylated), which are major and very specific components of the cell envelope of *M. tuberculosis* and play a crucial role in its remarkable architecture and impermeability (Daffé and Draper, 1998). Their biosynthesis is the target of the front-line and highly efficient antituberculous drug isoniazid (Takayama et al., 1972) and this pathway still represents an important reservoir of targets for the development of new antimycobacterial drugs. Many enzymes of the pathway have been discovered, among which are the enzymes of the fatty acid synthase II (FAS-II) system involved in the formation of the very long meromycolic chain (C_{50}–C_{60}), and the transferases that introduce methyl groups on this chain (for review, see Marrakchi et al., 2008). The ultimate step in the pathway, the "mycolic condensation" of two long-chain fatty acids, has been shown to require at least three enzymes encoded by the putative *accD4-pks13-fadD32* operon (Portevin et al., 2004, 2005). This gene cluster is restricted to mycolic-acid-producing bacterial species, the so-called *Corynebacterineae* suborder (Gande et al., 2004; Portevin et al., 2004, 2005). AccD4 and FadD32 play a role in the activation of the substrates of the condensing enzyme, Pks13, and all three proteins are essential for the viability of mycobacteria (Portevin et al., 2004, 2005). AccD4 is a subunit of the acyl-CoA carboxylase (ACC) complex that activates the α-branch of mycolates through a carboxylation step (Gande et al., 2007), whereas FadD32, a fatty acyl-AMP ligase (FAAL), catalyzes the formation of acyl-adenylates, proposed to be the "activated" form of the very long meromycolic acid substrate in the mycolic condensation reaction (Portevin et al., 2005; Trivedi et al., 2004). Finally, the reduction of the β-ketoacyl product formed after condensation by Pks13 is catalyzed by CmrA to yield the mature mycolic acids (Lea-Smith et al., 2007).

FadD32, one of the 34 FadD proteins of *M. tuberculosis* annotated as putative fatty acyl-CoA synthetases (FACS), is a member of the adenylate-forming enzyme superfamily PF00501 (Finn et al., 2008) that includes the acyl- and aryl-CoA synthetases or ligases, the adenylation domains of the nonribosomal peptide synthetases (NRPS), and firefly luciferases. In the two-step reaction catalyzed by enzymes of this superfamily, a carboxylated substrate is first activated with ATP, to form an acyl-adenylate (acyl-AMP) intermediate (Figure 1). In the second half-reaction, these enzymes catalyze the formation of thioester of either CoA or acyl-carrier protein (ACP) (Bar-Tana et al., 1972; Bar-Tana and Rose, 1973; Hisanaga et al., 2004). Based on their primary sequence similarity, which was found to correlate with their functions, the *M. tuberculosis* FadD proteins have been subdivided in two classes, namely, (i) a large group of FadD proteins displaying the expected FACS activity, and (ii) a small subset of FadD proteins, which includes FadD32, displaying solely the FAAL activity (i.e., catalyzing only the first half-reaction) (Figure 1) (Trivedi et al., 2004).

 ©2009 Elsevier Ltd All rights reserved

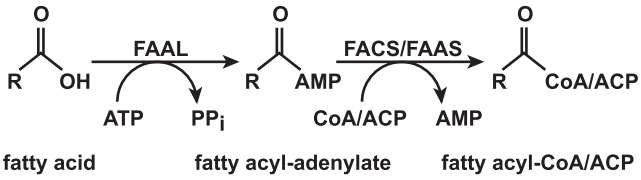

Figure 1. Two-Step Chemical Reaction Catalyzed by Acyl-CoA/ACP Synthetases

Fatty acyl-AMP ligases (FAAL) and fatty acyl-CoA or -ACP synthetases (FACS/FAAS) catalyze the formation of the acyl-adenylate intermediate; only FACS/FAAS are able to catalyze the second half reaction to yield fatty acyl CoA/ACP. R corresponds to alkyl chain (CH_3-$(CH_2)_n$-).

In the present study, we report the biochemical and kinetic characterization of the FAAL activity of FadD32. We also demonstrate the ability of the protein to further transfer the synthesized acyl-adenylate onto a thioester acceptor, an unrevealed acyl-ACP ligase function that shed light on the cross talk between some polyketide synthases and their associated adenylation enzymes. In addition, as a first step in the design of mechanism-based novel antimycobacterial agents, we synthesized a substrate analog and showed that it inhibits both FadD32 activity and mycolic acid synthesis, and affects mycobacterial survival.

RESULTS

Characteristic Features of FadD32

The analysis of the *Corynebacterineae* genomes sequenced so far revealed the strict conservation of the *fadD32* gene within the *accD4-pks13-fadD32* cluster, with the encoded proteins exhibiting high levels of sequence similarity (Portevin et al., 2005). It also underlined the requirement of the *fadD32*-encoded protein for mycolic acid biosynthesis, in agreement with the essentiality of the gene in mycobacteria (Portevin et al., 2005). The *fadD32* open reading frame specifies a protein from the ATP-dependent AMP-binding protein superfamily whose various members catalyze mechanistically similar two-step reactions (Figure 1). Alignment of the primary sequences of FadD32 with a set of proteins catalyzing the acylation reaction using diverse substrates revealed a few regions of high similarity and conserved signature motifs, A3 to A10 (according to the nomenclature adopted for the NRPS adenylation domains [Marahiel et al., 1997]), characteristic of these adenylate-forming proteins (Ingram-Smith et al., 2006; Morsczeck et al., 2001) (Figure 2). The crystal structures of the adenylate-forming enzymes (AFE) so far determined show that these proteins, despite their low sequence identities, uniformly adopt a similar fold and domain structure: a large N-terminal and a smaller C-terminal domain, with the active site residing at the interface between the two

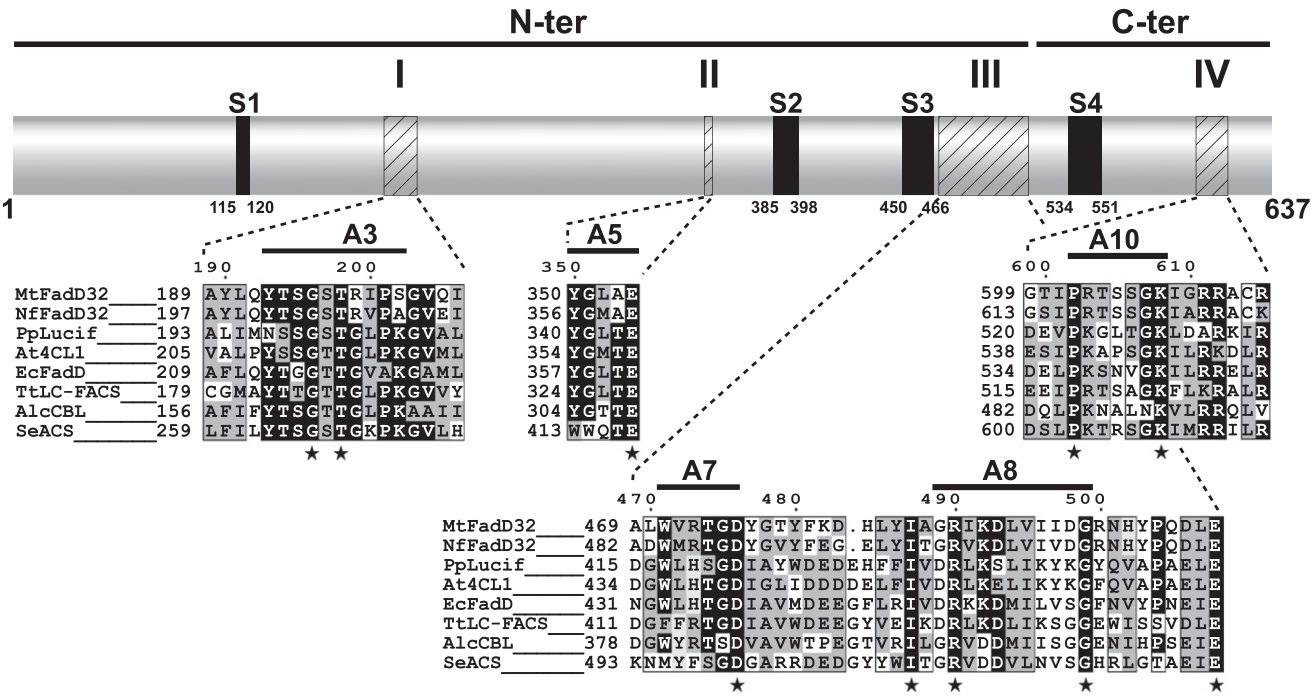

Figure 2. Conserved Motifs in FadD32 and Adenylate-Forming Proteins

Structure-based amino acid sequence alignment of the FadD32 (top row) with other members of the AMP-forming family. Regions corresponding to the conserved motifs I to IV are displayed as hatched boxes and the embedded highly conserved A3–A10 patches are delineated with solid lines above the sequences. Black boxes indicate amino acid stretches S1–S4 found only in FadD32 proteins. For sequences aligned, darker background corresponds to higher conservation and invariable residues are indicated by stars. MtFadD32 (*M. tuberculosis* FadD32, CAA17865); NfFadD32 (*Nocardia farcinica* FadD32, YP_116394); PpLucif (*Photinus pyralis* luciferase, BAF48396); At4CL1 (*Arabidopsis thaliana* 4-coumarate-CoA ligase, Q42524); EcFadD (*Escherichia coli* FadD, CAA50321); TtLC-FACS (*Thermus thermophilus* long-chain fatty acyl-CoA synthetase, BAD20228); AlcCBL (*Alcaligenes sp.* chlorobenzoate-CoA ligase, AAN10109); SeACS (*Salmonella enterica ser tiphymurium* acetyl-CoA synthetase, AAO71645).

domains (Conti et al., 1996, 1997; May et al., 2002; Reger et al., 2008).

Structure-based alignment of various AFE sequences, together with the predicted secondary elements of FadD32, revealed the presence of four additional stretches (S1 to S4) of amino acids of variable lengths (6–19 amino acids); S1–S3 being exclusively found in FadD32 proteins of all *Corynebacterineae* examined among other AFE (see Figure S1 available online and Figure 2). The two central insertions S2 and S3 surround the substrate binding pocket that comprises at least A3, A5, and A7 sequence motifs (in the N-terminal domain of the protein), whereas the two remaining insertions (S1 and S4) are in the close vicinity of the acceptor binding pocket and the A8 region. Finally, of potential importance is the long C-terminal insertion S4 following the A8-motif III (residues 534–551) that could be drawn from this structural alignment (Figure 2). This insertion is not only specific for FadD32 among the AFE, but also, and more importantly, is missing in the other FAAL enzymes of *M. tuberculosis* (e.g., FadD26) (Figure S1). Interestingly, S4 occurs in the FadD32 of all representatives of the genera of the *Corynebacterineae* suborder examined except *Corynebacterium* (Figure S1), a genus that produces the shortest (C_{32}–C_{36}) mycolic acids.

Expression and Purification of FadD32

The *fadD32* gene (*Rv3801c*) from *M. tuberculosis* was cloned and the encoded protein was produced either as a fusion with a cleavable amino- or carboxy-terminal hexa-histidine tag. Attempts to produce FadD32 with a C-terminal His-tag in a soluble form were unsuccessful. The production of the N-terminal-tagged FadD32 was induced in the *E. coli* BL21 (DE3) strain and purification by affinity chromatography followed by gel filtration chromatography allowed an enrichment of the protein with approximately a 50-fold increase in the specific activity of the pure protein over the crude extract (Figure S2). Depending on whether an imidazole- or a pH-gradient was used to elute the His-tagged FadD32 from the affinity column, distinct gel filtration elution profiles were obtained (Figure 3). In the elution using imidazole, the profile displayed two peaks, both of which contained FadD32, whereas a single major peak was obtained when the protein was eluted with a pH-gradient (Figure 3). Dynamic light scattering analysis and FAAL activity determination (see below) of the peaks indicated that the high-molecular-weight species (contained in peak 1, Figure 3), presumably induced by the presence of imidazole, did not exhibit FAAL activity. In contrast, the combined fractions from the second peak eluted with imidazole, as well as those of the single peak from the pH-gradient, displayed the FAAL activity (left inset of Figure 3). Consequently, a pH gradient was preferred for eluting His_6-FadD32 from the affinity column prior to gel filtration chromatography. SDS-PAGE and western blot analyses using antihistidine antibodies of the FadD32-containing fractions during purification steps indicated an essentially homogenous protein (Figure S2). The purified His_6-tagged FadD32 protein migrates on SDS-PAGE close to the predicted molecular mass (71,395 Da) (right inset of Figure 3). Consistently, size exclusion chromatography allowed estimation of the apparent molecular mass at about 71 kDa, suggesting that the active form of the protein is a monomer in solution (Figure S2).

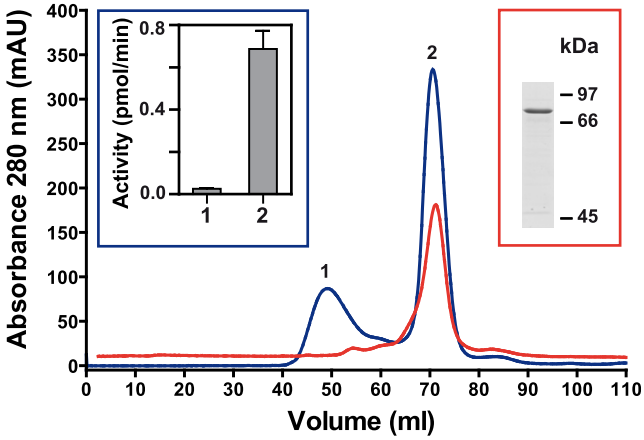

Figure 3. Purification, Activity, and Aggregation State of His_6-FadD32

Elution profile of His_6-FadD32 using a gel filtration (Superdex 200) column after a first step of affinity chromatography was performed using either an imidazole (blue trace) or pH gradient (red trace) for elution. Fatty acyl-AMP ligase (FAAL) activity in peaks 1 and 2 derived from the imidazole purification (left inset); means and standard error of the mean (SEM) of two replicates are shown, and data are representative of three independent experiments. Fractions from the Superdex 200 major peak obtained in the pH-gradient purification were pooled and analyzed by SDS-PAGE (right inset).

FadD32 Enzymatic Characterization and Substrate Specificity

The FAAL activity of the purified FadD32 was determined by radiolabeled-thin layer chromatography (radio-TLC) (Trivedi et al., 2004). The FadD32 protein was used to generate [^{14}C]acyl-AMP from [1-^{14}C]fatty acid; the substrate being subsequently separated from the product on the basis of their differential *Rf* (frontal ratio). In the presence of dodecanoic acid, a production of C12-AMP by FadD32 was observed and found to be both ATP- and Mg^{2+}-dependent (Figure 4A); expectedly, the presence of CoA in the mixture did not result in the production of acyl-CoA (Trivedi et al., 2004), demonstrating that the purified FadD32 possessed a FAAL activity in our in vitro assay. The FadD32 enzyme exhibited typical Michaelis-Menten profiles when its acyl-adenylation activity was determined using increasing concentrations of fatty acid (Figure S3). To determine the FadD32 FAAL-specific activity, the acyl-AMP formation as a function of enzyme concentration was measured (Figure 4B). The optimal conditions for the measurement of the initial velocity were determined (Figure S4). The response was linear in the range of FadD32 concentrations tested (up to 2.4 μM and 0.8 μM with C12 and C14 fatty acid substrates, respectively). Under standard assay conditions, the enzyme was much more active when C14 was used as substrate, compared with C12 (Figure 4B). The specific activities calculated for the enzyme (at 20 μM of substrate) were 0.32 ± 0.02 and 1.59 ± 0.21 nmol min^{-1} mg^{-1} protein for C12 and C14, respectively. It is worth noting that the value obtained in the presence of the latter substrate was similar to that of the *E. coli* fatty acyl-CoA synthetase FadK (1 nmol C14-CoA min^{-1} mg^{-1} [Morgan-Kiss and Cronan, 2004]).

To gain insight into the substrate specificity of FadD32, the protein was incubated with a panel of commercially available

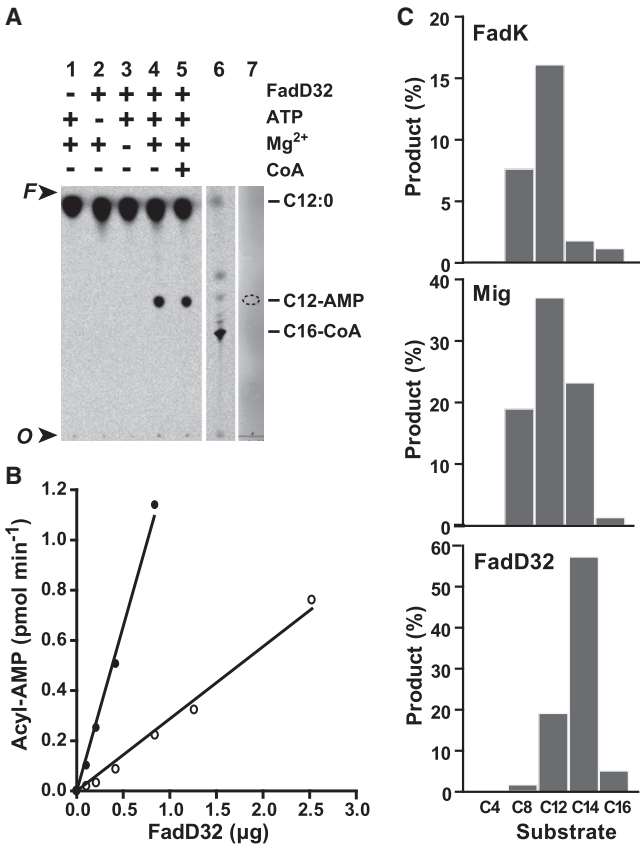

Figure 4. FadD32 Fatty Acyl-AMP Ligase (FAAL) Activity and Acyl Chain-Length Selectivity

(A) The FAAL activity and the requirements of FadD32. The assays contained the indicated components and were initiated either with the enzyme (2 μM) or with [1-^{14}C]C12:0 fatty acid (50 μM) in the minus-enzyme assay. The reaction products were separated by TLC and detected by autoradiography; migration origin (*O*) and front (*F*). The TLC profile shown is representative of two replicates. [^{14}C]C16-CoA (lane 6) and cold C12-AMP (lane 7) were used as standards; the latter synthetic product was detected after spraying the plate with rhodamine B and observation under UV (the spot was highlighted for clarity).

(B) Specific activity of FadD32 using either [1-^{14}C]C12:0 (○) or [1-^{14}C]C14:0 (●) as substrate.

(C) The enzymatic activities of His_6-FadK, His_6-Mig and His_6-FadD32 were determined in the presence of 20 μM of the indicated [1-^{14}C]fatty acids with different chain lengths. Incorporation of radioactivity into product, acyl-CoA (for FadK and Mig) or acyl-AMP (for FadD32), was displayed as percentages of the total radioactivity (including those contained in the spot [remained at the origin], substrate and product). The graph showing FadD32 selectivity is representative of two independent experiments.

radiolabeled fatty acids, from C4 to C16, and the acyl-adenylation activity was determined. The FadD32 substrate selectivity profile was compared with those of two FACS, namely the *E. coli* FadK and the *Mycobacterium avium* Mig, known to display, respectively, short-chain and medium-chain length specificity. The latter proteins were expressed and purified as described (Morgan-Kiss and Cronan, 2004; Morsczeck et al., 2001) and their FACS activity was tested in a typical FadD32 radio-TLC assay containing CoA and using [1-^{14}C]labeled fatty acids at a fixed concentration. Whereas FadK and Mig exhibited substrate preferences centered on C8-C12 and C8-C14 fatty acids, respectively, FadD32 was most active when C14 was used as substrate (Figure 4C).

In order to investigate further the enzymatic properties of FadD32, kinetic parameters for selected chain fatty acid substrates (C12, C14, and C16) were determined. FadD32 displayed typical Michaelis-Menten profiles (Figure S3) and converted C12:0, C14:0 and C16:0 to their respective acyl-adenylates, with the enzyme affinity and catalytic efficiency (k_{cat}/K_m) increasing with the chain length of the substrate (Table S1). Expectedly, FadD32 demonstrated the highest affinity (K_m of 3.2 μM) toward C16, 1000-fold increased as compared with that toward C12. In terms of catalytic efficiencies, the C16 and C14 represented the most efficiently converted substrates, with k_{cat}/K_m of 4.7 and 6.2 mM^{-1} min^{-1}, respectively; 80- to 100-fold higher than that for C12 (Table S1). The apparent activity of the enzyme with C4 and C8 was too low for activity determination in the standard FAAL assay. The purified FadD32 showed a K_m of 2 mM for ATP (Table S1), which is in the same order of magnitude of those described for other FACS (Hall et al., 2005; Rusnak et al., 1989). Thus, determination of FadD32 catalytic constants for substrates indicated again that the protein displays a preference for long-chain over medium- and short-chain fatty acid substrates.

To assess the specificity of FadD32 for longer substrates, a competitive kinetic assay was performed because of the unavailability of commercially radiolabeled fatty acids longer than C20. The competing long- and very long-chain fatty acids were added at a fixed concentration to the reaction containing increasing concentrations of [^{14}C]substrate (Figure S5); C16 was chosen for these experiments, based on the high affinity of the enzyme toward this substrate (see above). The formation of C16-AMP by FadD32 as a function of [^{14}C]C16 concentration in the absence or presence of cold C16 showed typical curves of efficient competitive binding (Figure S5). Unexpectedly, however, the addition of 10 μM C20 or C24 resulted in binding curves with higher rate (V_{max}) values than the control without competitor (Figure S5). This reproducible observation suggested the occurrence of an underlying phenomenon, reminiscent of a "detergent" effect, probably due to the long aliphatic chains of the competitors tested. Consistently, the addition of low concentrations (0.1%) of Triton X-100 to FadD32 assays significantly improved the enzyme activity (Figure S5). Further attempts to improve the experimental conditions for these competitive binding assays in order to dissect the effect of long-chain substrates on FadD32 activity were unsuccessful.

Structural Features of FadD32 Suggestive of an Additional Acylation Activity

From structural and biochemical studies with acetyl-CoA synthetase (Acs) and chlorobenzoyl-CoA ligase (CBL) (Reger et al., 2007, 2008), the adenylate-forming enzymes have been proposed to have a "domain alternation" type of catalysis, where conformational changes take place and define either an adenylate- or a thioester-forming conformation, the two conformational states being in equilibrium. The role of the domain movement would be to remove stabilizing residues that are necessary for the adenylation half-reaction from the active site and simultaneously create a binding pocket for the phosphopantetheine (P-pant) of the acceptor. Key residues involved in both

conformations are found conserved in FadD32 (Figure 2), with the Lys608 (in A10-motif IV) essential for the adenylate-forming conformation and Gly499 (in A8-motif III), ensuring the thioester-forming conformation by hydrogen bonding to the P-pant moiety, as shown for Acs and CBL (Reger et al., 2007, 2008). Importantly, the conservation of this glycine in FadD32 was suggestive of the enzyme acylation activity (acyl-CoA/ACP) because kinetic analysis of an Acs mutant in this residue (Gly to Leu) was only active for the adenylate-forming half-reaction (Reger et al., 2007). Thus, the alignment of FadD32 with acyl-adenylate-forming enzymes (Figure 2) suggested that the protein would catalyze the two half-reactions usually performed by FACS and fatty acyl-ACP synthetase (FAAS) enzymes (Figure 1). In addition, as stated above, the exclusive occurrence of the long C-terminal insertion S4 following the A8-motif III (Figure 2) in FadD32 among both the AFE and the other FAAL of *M. tuberculosis* FadD points to the potential interaction of FadD32 with the P-pant moiety of an "acceptor" molecule/domain and to specific features of the protein of possible importance in catalysis and/or substrate specificity.

FadD32 Displays Acyl-ACP Synthetase Activity

To investigate the possible acylation activity of FadD32 and determine its "acceptor" selectivity, several substrates (CoA, ACP, AcpM, Pks13) were tested in modified FAAL, FACS, and FAAS assays using FadD32 or control enzymes, i.e., *E. coli* FadK (a FACS enzyme) and Aas (a FAAS protein), purified as described previously (Morgan-Kiss and Cronan, 2004; Shanklin, 2000). In the presence of CoA, FadD32, unlike FadK, was unable to convert the C14-AMP (formed from [1-^{14}C]C14 and ATP) to the corresponding acyl-CoA (Figure 5C, lanes 3 and 4), as expected (Trivedi et al., 2004). To investigate whether FadD32 could acylate ACP, the enzyme was mixed with either *E. coli* holo-ACP or *M. tuberculosis* holo-ACP (holo-AcpM) and the formation of labeled C14-ACP was analyzed by conformationally sensitive gel electrophoresis (Post-Beittenmiller et al., 1991; Rock et al., 1981) (Figure 5A). In the presence of holo-ACP, no acyl-ACP was detected when FadD32 was used in the assay, unlike the high acyl-ACP synthetase activity observed with Aas (Figure 5A, lanes 2 and 3). In contrast, in the presence of AcpM, FadD32 showed a significant acylation activity, as demonstrated by the formation of labeled acyl-AcpM, comparable to that measured for the acyl-ACP synthetase Aas in the presence of holo-AcpM (Figure 5A lower panel, lanes 4 and 5). Finally, the radiolabeling associated with the Pks13 protein (Figure 5B, lower panel, lane 3), likely due to the transfer of [^{14}C]acyl chain from the intermediate C14-AMP onto the protein, was specifically observed in the presence of FadD32, but not in that of Aas (Figure 5B, lanes 2 and 3). These data demonstrated that, in addition to its FAAL activity, FadD32 functions as an acyl-ACP ligase in vitro and that this acylation activity is highly specific and restricted to a limited number of "acceptors," namely, AcpM and the condensing enzyme Pks13, the latter being probably the natural and most efficient substrate.

In order to investigate the molecular basis of the FadD32 specificity toward ACPs from different sources, a bioinformatic analysis was performed (Figure 6). Alignment of *E. coli* ACP and AcpM indicates a high degree of similarity between the proteins, especially in the four-helix bundle ACP fold (residues

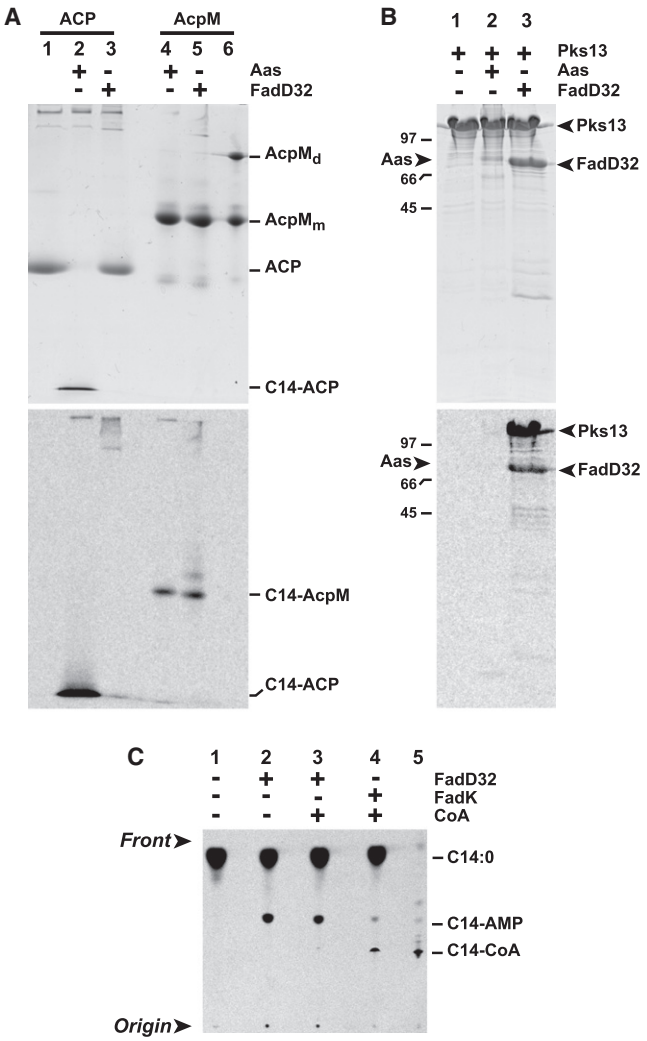

Figure 5. Determination of the Acceptor Selectivity of FadD32 In Vitro

All reactions used [1-^{14}C]C14:0 as substrate in a standard FAAL, FACS, or FAAS assay.

(A) The FadD32 acylation activity in the presence of either *E. coli* holo-ACP or *M. tuberculosis* holo-AcpM was analyzed by urea-PAGE (2.5 M, 15%) (Post-Beittenmiller et al., 1991; Rock et al., 1981). The assays included Aas (1 μM) or FadD32 (4 μM); lane 1 contains holo-ACP and lane 6, holo-AcpM (with the two distinctive bands that correspond to the monomer [AcpM$_m$] and disulfide dimer [AcpM$_d$]).

(B) Loading of the labeled acyl chain from C14-AMP (generated using either Aas [0.6 μM] or FadD32 [2.1 μM]) onto Pks13 (3.6 μM) analyzed by SDS-PAGE. Detection in (A) and (B) was by Coomassie staining and by autoradiography in upper and lower panels, respectively.

(C) Radio-TLC analysis of FadD32 products using CoA as acceptor. The *E. coli* FadK, a FACS, was used as a control for the synthesis of acyl-CoA (lane 4); both enzymes were added at 2.1 μM, and lane 5 contained a [^{14}C]C16-CoA standard.

1–82) at their N termini, while the particularity of AcpM resides in an extended carboxyl-terminus (residues 83–115). Strikingly, the N-ACP (amino-terminal ACP) domain of Pks13, onto which the transfer of the acyl chain from FadD32 to the condensase has been suggested to occur (Trivedi et al., 2004), also displays such an extension. Despite the relatively low degree of similarity

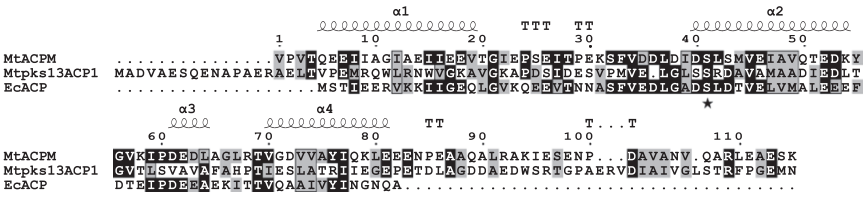

Figure 6. Structure-Based Amino Acid Sequence Alignment of ACPs

The four-helix bundle characteristic of the ACP fold is displayed for AcpM (Wong et al., 2002). Black and gray shadings indicate strictly conserved and similar residues, respectively, and a star indicates the conserved serine residue where the prosthetic group binds. MtAcpM (*M. tuberculosis* AcpM, CAA94640); Mtpks13ACP1(N-terminal ACP domain of *M. tuberculosis* Pks13, CAA17864); EcACP (*E. coli* ACP, AAB27925).

between the two C-terminal extensions, AcpM and the N-ACP domain of Pks13 sequences align quite well (Figure 6), suggesting that this common feature very likely plays a role in determining the specificity of the FadD32-acceptor interaction.

Inhibition of FadD32 Activity

The ultimate goal of identifying and characterizing essential and specific proteins of the tubercle bacillus is their use as novel targets for the development of new antituberculous drugs. FadD32 is one of these newly discovered candidates (Portevin et al., 2005). Various nonhydrolyzable acyl-AMP analogs have been recently used as mechanism-based inhibitors, which were found to be potent inhibitors of related adenylate-forming enzymes (Arora et al., 2009; Ferreras et al., 2005, 2008). Adenosine 5′-alkyl phosphates, are structural analogs of adenosine 5′-acyl phosphates (acyl-AMP) (Figure 7A, **(1)**), the transient intermediates of the acyl-CoA/ACP synthetic reaction (Figure 1). Based on these considerations, we postulated that the reaction intermediate mimic adenosine 5′-dodecylphosphate (alkyl-adenylate, AMPC12, Figure 7A **(2)**), known to inhibit many FACS (Grayson and Westkaemper, 1988; Shiraishi et al., 1994), would be a potent inhibitor of the acyl-adenylation activity of FadD32. We chemically synthesized AMPC12 as described previously (Machida et al., 1997) and checked its structure by mass spectrometry and nuclear magnetic resonance (see Supplemental Data). We first tested the inhibitory effect of the synthesized alkyl phosphate on the acyl-CoA synthetase FadK from *E. coli*. In a typical acyl-AMP ligase assay containing [1-^{14}C]fatty acid and CoA as substrates, AMPC12 showed a significant inhibition on the FadK activity (85% of the original level at 2 μM). The inhibitory effect of the AMPC12 on FadD32 activity was then examined by varying the inhibitor concentration (0.05–10 μM) at a fixed concentration (100 μM) of the fatty acid substrate ([^{14}C]C14). As shown in Figure 7B, the AMP analog inhibited the activity of the enzyme in a concentration-dependent manner, reducing it by almost 90% of the original level at 2 μM, remarkably comparable to the effect of the inhibitor on FadK. The calculated half-maximal effective concentration (EC_{50}) of the AMPC12 compound corresponds to 0.11 μM, which is less than 20 times the enzyme concentration used in the assay. Because the AMPC12 was active on FadD32, we investigated whether this AMP analog could influence the mycobacterial growth. For this purpose, *Mycobacterium smegmatis* mc^{2}155 cells (OD_{600} of 0.02) were incubated in 96-well plates at 37°C in the presence of increasing concentrations (8–75 μM) of AMPC12 and their viability was monitored after 48 hr using the tetrazolium salt assay (Sieuwerts et al., 1995). The same concentrations of AMPC12 were tested in parallel on growing cells of *Corynebacterium glutamicum* and *E. coli*. The addition of AMPC12 to *M. smegmatis* induced a dose-dependent inhibition of growth with more than 80% loss of viability at 19 μM of the inhibitor (Figure 7C). At this concentration, about 45% growth impairment of *C. glutamicum* was observed whereas *E. coli* was almost insensitive to AMPC12. Because *M. smegmatis* and *C. glutamicum* were the most sensitive to AMPC12, we hypothesized that these mycolic-acid-synthesizing bacteria have their mycolic acid metabolism affected by the synthetic analog. We therefore examined the inhibitory effect of AMPC12 on fatty acid/mycolic acid synthesis in *M. smegmatis* using a cell-free extract (CFE) synthesizing most exclusively mycolic acids (Lacave et al., 1990). AMPC12 was pre-incubated with CFE for 30 min and the synthesis of [1-^{14}C]acetate-labeled fatty acids and mycolic acids was allowed for 60 min before lipids were extracted and analyzed. Although no effect on fatty acid synthesis was observed at a subinhibitory concentration of AMPC12 (10 μM), an inhibition of 40% of the synthesis of all types of *M. smegmatis* mycolic acids (alpha, alpha′, epoxy) was observed (data not shown). These results indicated that AMPC12 could reach its target within the particular system of CFE and that inhibition of mycolic acid synthesis occurs very likely through the inhibition of FadD32 activity.

DISCUSSION

The present study was undertaken in order to characterize the enzymatic properties of FadD32, a protein essential for mycolic acid synthesis, and define its substrate specificity. From its chromatographic behavior, the His_6-FadD32 appeared active as a monomer in solution. It is unknown, however, whether FadD32 exists as a monomer in the "condensing complex" in vivo where it possibly engages interaction(s) with its partners, Pks13 and AccD4. Expectedly, the purified FadD32 possessed an acyl-AMP ligase activity in vitro and was able to synthesize acyl-adenylates from fatty acids and ATP in the presence of Mg^{2+}. Investigation of detailed kinetic properties of the enzyme showed that FadD32 exhibited the strongest affinity toward C16 fatty acid and best catalytic efficiencies toward C16:0 and C14:0 acids. These properties distinguish FadD32 from the (middle-chain) acyl-CoA synthetase Mig of *M. avium*, whose substrate specificity is centered on C10 (Morsczeck et al., 2001). FadD32 thus presents an apparent selectivity profile centered on C14-C16 and can be classified as a long-chain acyl-AMP ligase in vitro. For a matter of unavailability of very long-chain radiolabeled molecules, we used cold fatty acids in a competitive kinetic assay to investigate the specificity of FadD32 for very long-chain substrates (Figure S5). Because a "detergent" effect was invariably observed in the presence

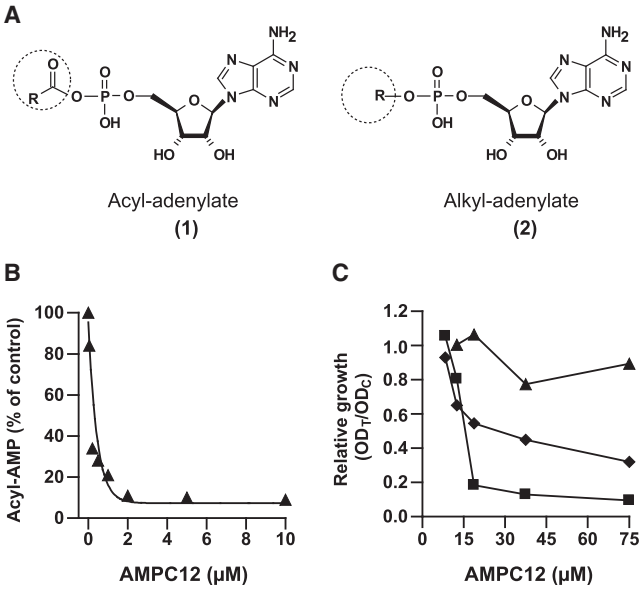

Figure 7. Inhibitory Effect of Dodecyl-AMP (AMPC12) on FadD32 Activity and on Bacterial Growth

(A) Chemical structures of acyl-adenylate intermediate (acyl-AMP, (**1**)) and its analog, adenosine 5′-alkylphosphate (alkyl-AMP, AMPC12, (**2**)), R = C12.

(B) FadD32 activity in the presence of increasing concentrations of AMPC12 was determined in a typical radio-TLC assay (using 100 μM [1-^{14}C]C14:0 as substrate and 2.1 μM enzyme). Data shown are representative of two independent experiments.

(C) Bacterial growth inhibition curves of *M. smegmatis* mc^{2}155 (■), *C. glutamicum* ATCC13032 (◆), and *E. coli* DH5α (▲) strains in the presence of increasing concentrations of AMPC12 were determined. OD$_T$/OD$_C$, ratio of OD$_{580nm}$ of inhibitor-treated (OD$_T$) to OD$_{580nm}$ of control cultures (OD$_C$), DMSO-treated. Data show the mean of two replicates.

of fatty acids longer than C20, the specificity of FadD32 could not be studied in the presence of its presumed natural substrates in mycobacteria, i.e., C_{54}–C_{64} meromycolic acids. Compared with specific activities described for short- or medium-chain FACS from the same family (*S. enterica* Acs [Ingram-Smith et al., 2006], *E. coli* FadD [Morgan-Kiss and Cronan, 2004], *M. avium* Mig [Morsczeck et al., 2001]), the *M. tuberculosis* FadD32 exhibits a relatively low activity toward middle- to long-chain substrates (C12–C16), which probably reflects the low catalytic efficiency of the protein in the presence of these relatively "short" substrates as compared with the natural substrates. Elements from amino acid alignment of FadD32 with other AMP-forming proteins and short-chain acyl-CoA synthetases corroborate this result (Figure 2). Indeed, among the specific amino acid residues shown to be involved in chain length selectivity of proteins from this superfamily (Black et al., 1997; Ingram-Smith et al., 2006) is a Gly that is present in FadD32 (Gly351 in motif II, Figure 2), whereas in the aligned sequence of the *S. enterica* short-chain acyl-CoA synthetase Acs, a Trp is found in lieu of the Gly residue. Interestingly, in the case of the *S. enterica* Acs that has a preference for acetate and propionate, the removal of the equivalent Trp416 side chain from the hydrophobic pocket was sufficient to enlarge the pocket to accommodate longer substrates (Ingram-Smith et al., 2006).

The very-long-chain acyl-adenylates produced by FadD32 are the putative activated substrates for the condensation reaction catalyzed by Pks13. The resulting meromycoloyl chains should then be transferred onto the N-ACP domain of Pks13 by either a yet unknown enzyme or FadD32 that would then necessarily possess an unrevealed additional function (Gavalda et al., 2009). Investigation of the putative additional acyl-ACP synthetase function of FadD32 led to the demonstration that the enzyme is also able to acylate the mycobacterial AcpM. Thus, FadD32 would not simply be a "fatty acyl-AMP ligase," as previously suggested (Trivedi et al., 2004), but rather would catalyze the two half-reactions usually performed by FadD enzymes, i.e., the production of an acyl-AMP from a fatty acid and ATP, then the transfer of the acyl chain from the acyl-AMP onto the P-pant moiety of a substrate, the natural one being in the present case Pks13. It is noteworthy that among the 12 FadD proteins of *M. tuberculosis* previously classified as FAAL (Trivedi et al., 2004), 9 have their gene located near a *pks* that includes an *acp* sequence or near an *acp*-like gene (Table S2). The enzymes belonging to this subfamily are likely to have the function of producing ACP/PCP (peptidyl carrier protein) derivatives. Thus, with respect to their substrate specificity, FadD enzymes would either synthesize acyl-CoA or acyl-ACP/PCP molecules, the ACP or PCP being either free-standing proteins or PKS- and NRPS-associated domains. It is noteworthy that Cronan's group has recently reported the characterization of an acyl-ACP synthetase from *Vibrio harveyi* that was previously classified as a member of the acyl-CoA synthetase family (Jiang et al., 2006). In this regard, FadD32 would be a prototype of the *M. tuberculosis* FadD proteins classified as FAAL, where these adenylate-forming enzymes associated to *pks* genes would catalyze ACP-acylation reactions. In agreement with this hypothesis, we have observed that another FadD protein, namely FadD26, also possesses an acyl-ACP activity (our unpublished data).

As an acyl-ACP synthetase, FadD32 is capable of acylating the mycobacterial AcpM but neither ACP from *E. coli* nor CoA, the N-terminal domain of Pks13 being its very likely natural and highly specific in vivo acceptor. These results strongly suggest that specific features of AcpM *versus E. coli* ACP and/or specificity of the interaction FadD32-acceptor domain might be involved. This assumption was further supported by the bioinformatic analysis of ACP from different sources. The alignment of the protein sequences shows a high degree of similarity at their N termini, yet AcpM has an extended carboxyl-terminus that aligns quite well with the sequence of the N-ACP domain of Pks13 despite their low degree of similarity. This suggests that this common feature very likely plays a role in determining the molecular basis underlying the chain-length specificity of fatty acyl intermediates during mycolic acid biosynthesis.

Finally, as a first step in the validation of FadD32 as a good target for the search of new antituberculous drug, we showed that the alkylphosphate ester of AMP, adenosine 5′-dodecylphosphate (AMPC12), inhibited the acyl-AMP ligase activity of FadD32. This reasoning was based on the observed inhibition of many FACS by this molecule. This compound has a structure analogous to acyl-AMP, the transient intermediate of the acyl-CoA/ACP synthetic reaction (Figure 1). Furthermore, AMP analogs were recently reported as potent inhibitors of acyl- and aryl-adenylation domains of enzymes involved in the production

 ©2009 Elsevier Ltd All rights reserved

of some mycobacterial lipids (Arora et al., 2009; Ferreras et al., 2005, 2008). Indeed, AMPC12, which also inhibited both mycolic acid synthesis and mycobacterial growth, is an efficient inhibitor of FadD32. Based on the inhibition data presented herein, AMPC12 represents a promising tool for the study of substrate binding pocket and three-dimensional structure determination in complex with FadD32. Further insights into the enzymatic mechanism will require the structure determination of enzyme-ligand complexes to search for efficient inhibitors in the perspective of antimycobacterial drug development.

SIGNIFICANCE

Mycolic acids are major and specific lipid components of the mycobacterial cell envelope, and essential for the survival of members of the genus, which contains numerous human and animal pathogens. Understanding the biosynthesis of these critical determinants of both the mycobacterial permeability and virulence is an important goal, because it might lead to design of new antituberculous drugs. FadD32 is an FAAL that activates the very long meromycolic acid (C_{50}–C_{60}) condensed by Pks13 with a C_{22}–C_{26} fatty acid to yield, after reduction, mycolic acids. The findings reported here demonstrate the biochemical and enzymatic properties of FadD32 and show that, in addition to the previously recognized FAAL activity, the protein possesses an acyl-ACP ligase function. Moreover, to the best of our knowledge, FadD32 is the first *M. tuberculosis* FAAL reported to possess such an activity and might be the prototype of a group of polyketide-synthase-associated adenylation enzymes with an uncommon catalytic mechanism. The substrate analog dodecyl-AMP efficiently inhibited the FadD32 activity, mycolic acid biosynthesis and mycobacterial growth. Overall, these studies advance our understanding of the biosynthesis of the hallmark of mycobacteria and open an avenue for the development of mechanism-based novel antimycobacterial agents.

EXPERIMENTAL PROCEDURES

Bioinformatic Sequence Analysis

Amino acid sequences were obtained from the National Center for Biotechnology Information. Alignments were performed using the Clustal W2 program (Larkin et al., 2007) and manually adjusted in Seaview (Galtier et al., 1996); the figures were shaped using Espript (Gouet et al., 1999).

Cloning and Purification of FadD32 (His_6-FadD32)

The cloning and purification of FadD32 are described in detail in the Supplemental Data. Briefly, the *M. tuberculosis* H37Rv *fadD32* gene was amplified by polymerase chain reaction and the insert was ligated into the pET15b *E. coli* expression vector (Novagen). The FadD32 expression was induced 5 hr at 25°C in *E. coli* BL21(DE3) cells. The cleared lysate expressing FadD32 was applied to HisTrap HP affinity column and elution of the protein was performed using either an imidazole or pH gradient. The FadD32-containing fractions were applied to a gel filtration chromatography (Superdex 200) column; the protein was homogeneous as judged by SDS-PAGE (Laemmli, 1970) and western blot analysis using anti-polyHis antibodies (detailed in Supplemental Data).

Enzymatic Assays for Acyl-AMP/ACP Ligase Activity

Enzymatic activity was determined by monitoring acyl-AMP formation using radio- TLC in which labeled fatty acid in the presence of ATP was converted into acyl-AMP that was separated from the substrate by TLC and detected by autoradiography (Trivedi et al., 2004). The standard FAAL reaction mixture included 100 mM Tris-HCl (pH 7), 20–100 μM [^{14}C]fatty acid, 2 mM ATP, 8 mM $MgCl_2$ and 0.2–3.6 μg protein in a 15 μl reaction volume. In the case of determination of FACS activity, 2 mM CoA was added to the mixture. The reaction, performed for 10 min at 30°C, was initiated by the addition of the enzyme, terminated by the addition of 5% acetic acid, and spotted on silica gel TLC plates (G60). Radiolabeled products were resolved in butan-1-ol/acetic acid/water (80:25:40) at room temperature and visualized by exposing the TLC to Fujifilm imaging plate prior to phosphorimager detection (Typhoon Trio GE Healthcare). A standard curve of labeled [^{14}C]fatty acid substrate allowed [^{14}C]acyl-AMP quantification using the ImageQuant software version 5.1 (Molecular Dynamics).

For FAAS/ligase activity determination, the reaction mixture (15 μl) contained 100 μM [1-^{14}C]C14 fatty acid, 2 mM DTT, 10 mM $MgCl_2$, 5 mM ATP in 100 mM Tris-HCl (pH 7), and 15–25 μM of ACP or AcpM, the latter being produced and purified as reported (Kremer et al., 2000). Reactions were started with the addition of enzyme and incubated for 2 hr at 30°C. For acyl-ACP and acyl-AcpM detection, 10–15 μl of reactions were analyzed by urea-PAGE (15% polyacrylamide gel containing 2.5 M urea [Kremer et al., 2000; Post-Beittenmiller et al., 1991; Rock et al., 1981]). To test the loading of the acyl chain from acyl-AMP (generated by FadD32) onto the Pks13 protein (purified as reported in Gavalda et al., 2009), the same reaction mixture was used except for the buffer (100 mM HEPES [pH 7] replaced Tris buffer); separation was performed by 12% SDS-PAGE. The labeled products were detected using phosphorimager.

Mycolic Acid Synthesis Assay and Analysis

The CFE synthesizing mycolic acids was prepared from *M. smegmatis* mc^2155 as described (Lacave et al., 1990). AMPC12 was added to the CFE for 30 min and the neosynthesis of fatty acids, including mycolic acids, was followed by the addition of 50 μm of [1-^{14}C]acetate as a precursor. The reaction was stopped 60 min later by saponification and lipids were extracted with diethyl ether. The effect of the AMPC12 on the incorporation of radioactivity into non-hydroxylated fatty acid methyl esters and mycolic acid methyl esters was determined.

SUPPLEMENTAL DATA

Supplemental Data include Supplemental Experimental Procedures, five figures, and two tables and can be found with this article online at http://www.cell.com/chemistry-biology/supplemental/S1074-5521(09)00147-1.

ACKNOWLEDGMENTS

The authors are grateful to A. Lemassu, F. Laval, P. Constant, and F. Bardou (IPBS) for their precious advice and help. We thank N. Eynard (IPBS) for fruitful discussions, F-X. Chauviac for technical help in the beginning of this work, and F. Viala for help with figure preparation. We also thank J.E. Cronan (University of Illinois), G. Plum (University of Köln), Y-M. Zhang (St Jude Children's Research Hospital), and J. Shanklin (Brookhaven National Laboratory) for kindly supplying the *fadK, mig, acpM,* and *aas* expression plasmids, respectively. This work was supported by the Centre National de la Recherche Scientifique (France), notably through the postdoctoral fellowships to S.G. and B.v.d.R., by the Université Paul Sabatier (Toulouse, France), and by the European Community New Medicines for Tuberculosis (grants LSHP-CT-2005-018923 and LSHP-CT-2006-037217).

Received: February 10, 2009
Revised: March 17, 2009
Accepted: March 23, 2009
Published: May 28, 2009

REFERENCES

Arora, P., Goyal, A., Natarajan, V.T., Rajakumara, E., Verma, P., Gupta, R., Yousuf, M., Trivedi, O.A., Mohanty, D., Tyagi, A., et al. (2009). Mechanistic

and functional insights into fatty acid activation in Mycobacterium tuberculosis. Nat. Chem. Biol. *3*, 166–173.

Bar-Tana, J., and Rose, G. (1973). Rat liver microsomal palmitoyl-coenzyme A synthetase. Structural properties. Biochem. J. *131*, 443–449.

Bar-Tana, J., Rose, G., and Shapiro, B. (1972). Microsomal palmitoyl coenzyme A synthetase from rat liver. Partial and exchange reactions. Biochem. J. *129*, 1101–1107.

Black, P.N., Zhang, Q., Weimar, J.D., and DiRusso, C.C. (1997). Mutational analysis of a fatty acyl-coenzyme A synthetase signature motif identifies seven amino acid residues that modulate fatty acid substrate specificity. J. Biol. Chem. *272*, 4896–4903.

Conti, E., Franks, N.P., and Brick, P. (1996). Crystal structure of firefly luciferase throws light on a superfamily of adenylate-forming enzymes. Structure *4*, 287–298.

Conti, E., Stachelhaus, T., Marahiel, M.A., and Brick, P. (1997). Structural basis for the activation of phenylalanine in the non-ribosomal biosynthesis of gramicidin S. EMBO J. *16*, 4174–4183.

Daffé, M., and Draper, P. (1998). The envelope layers of mycobacteria with reference to their pathogenicity. Adv. Microb. Physiol. *39*, 131–203.

Ferreras, J.A., Ryu, J.S., Di Lello, F., Tan, D.S., and Quadri, L.E. (2005). Small-molecule inhibition of siderophore biosynthesis in *Mycobacterium tuberculosis* and *Yersinia pestis*. Nat. Chem. Biol. *1*, 29–32.

Ferreras, J.A., Stirrett, K.L., Lu, X., Ryu, J.S., Soll, C.E., Tan, D.S., and Quadri, L.E. (2008). Mycobacterial phenolic glycolipid virulence factor biosynthesis: mechanism and small-molecule inhibition of polyketide chain initiation. Chem. Biol. *15*, 51–61.

Finn, R.D., Tate, J., Mistry, J., Coggill, P.C., Sammut, S.J., Hotz, H.R., Ceric, G., Forslund, K., Eddy, S.R., Sonnhammer, E.L., and Bateman, A. (2008). The Pfam protein families database. Nucleic Acids Res. *36*, D281–D288.

Galtier, N., Gouy, M., and Gautier, C. (1996). SEAVIEW and PHYLO_WIN: two graphic tools for sequence alignment and molecular phylogeny. Comput. Appl. Biosci. *12*, 543–548.

Gande, R., Gibson, K.J., Brown, A.K., Krumbach, K., Dover, L.G., Sahm, H., Shioyama, S., Oikawa, T., Besra, G.S., and Eggeling, L. (2004). Acyl-CoA carboxylases (*accD2* and *accD3*), together with a unique polyketide synthase (*Cg-pks*), are key to mycolic acid biosynthesis in *Corynebacterineae* such as *Corynebacterium glutamicum* and *Mycobacterium tuberculosis*. J. Biol. Chem. *279*, 44847–44857.

Gande, R., Dover, L.G., Krumbach, K., Besra, G.S., Sahm, H., Oikawa, T., and Eggeling, L. (2007). The two carboxylases of *Corynebacterium glutamicum* essential for fatty acid and mycolic acid synthesis. J. Bacteriol. *189*, 5257–5264.

Gavalda, S., Leger, M., van der Rest, B., Stella, A., Bardou, F., Montrozier, H., Chalut, C., Burlet-Schiltz, O., Marrakchi, H., Daffé, M., and Quémard, A. (2009). The Pks13/FadD32 crosstalk for the biosynthesis of mycolic acids in *Mycobacterium tuberculosis*. J. Biol. Chem., in press. Published online May 12 2009. 10.1074/jbc.M109.00640.

Gouet, P., Courcelle, E., Stuart, D.I., and Metoz, F. (1999). ESPript: analysis of multiple sequence alignments in PostScript. Bioinformatics *15*, 305–308.

Grayson, N.A., and Westkaemper, R.B. (1988). Stable analogs of acyl adenylates. Inhibition of acetyl- and acyl-CoA synthetase by adenosine 5′-alkylphosphates. Life Sci. *43*, 437–444.

Hall, A.M., Wiczer, B.M., Herrmann, T., Stremmel, W., and Bernlohr, D.A. (2005). Enzymatic properties of purified murine fatty acid transport protein 4 and analysis of acyl-CoA synthetase activities in tissues from FATP4 null mice. J. Biol. Chem. *280*, 11948–11954.

Hisanaga, Y., Ago, H., Nakagawa, N., Hamada, K., Ida, K., Yamamoto, M., Hori, T., Arii, Y., Sugahara, M., Kuramitsu, S., et al. (2004). Structural basis of the substrate-specific two-step catalysis of long chain fatty acyl-CoA synthetase dimer. J. Biol. Chem. *279*, 31717–31726.

Ingram-Smith, C., Woods, B.I., and Smith, K.S. (2006). Characterization of the acyl substrate binding pocket of acetyl-CoA synthetase. Biochemistry *45*, 11482–11490.

Jiang, Y., Chan, C.H., and Cronan, J.E. (2006). The soluble acyl-acyl carrier protein synthetase of *Vibrio harveyi* B392 is a member of the medium chain acyl-CoA synthetase family. Biochemistry *45*, 10008–10019.

Kremer, L., Baulard, A.R., and Besra, G.S. (2000). Genetics of mycolic acid biosynthesis. In Molecular Genetics of Mycobacteria, G.F. Hatfull and W.R. Jacobs, eds. (Washington, D.C.: ASM Press), pp. 173–190.

Lacave, C., Quemard, A., and Laneelle, G. (1990). Cell-free synthesis of mycolic acids in *Mycobacterium aurum*: radioactivity distribution in newly synthesized acids and presence of cell wall in the system. Biochim. Biophys. Acta *1045*, 58–68.

Laemmli, U.K. (1970). Cleavage of structural proteins during the assembly of the head of bacteriophage T4. Nature *227*, 680–685.

Larkin, M.A., Blackshields, G., Brown, N.P., Chenna, R., McGettigan, P.A., McWilliam, H., Valentin, F., Wallace, I.M., Wilm, A., Lopez, R., et al. (2007). Clustal W and Clustal X version 2.0. Bioinformatics *23*, 2947–2948.

Lea-Smith, D.J., Pyke, J.S., Tull, D., McConville, M.J., Coppel, R.L., and Crellin, P.K. (2007). The reductase that catalyzes mycolic motif synthesis is required for efficient attachment of mycolic acids to arabinogalactan. J. Biol. Chem. *282*, 11000–11008.

Machida, K., Tanaka, T., Shibata, K., and Taniguchi, M. (1997). Inhibitory effects of nucleoside 5′-alkylphosphates on sexual agglutination in *Saccharomyces cerevisiae*. FEMS Microbiol. Lett. *147*, 17–22.

Marahiel, M.A., Stachelhaus, T., and Mootz, H.D. (1997). Modular Peptide Synthetases Involved in Nonribosomal Peptide Synthesis. Chem. Rev. *97*, 2651–2674.

Marrakchi, H., Bardou, F., Laneelle, M., and Daffé, M. (2008). A Comprehensive Overview of Mycolic Acid Structure and Biosynthesis. In The Mycobacterial Cell Envelope, M. Daffé and J.M. Reyrat, eds. (Washington, DC: ASM Press), pp. 41–62.

May, J.J., Kessler, N., Marahiel, M.A., and Stubbs, M.T. (2002). Crystal structure of DhbE, an archetype for aryl acid activating domains of modular nonribosomal peptide synthetases. Proc. Natl. Acad. Sci. USA *99*, 12120–12125.

Morgan-Kiss, R.M., and Cronan, J.E. (2004). The *Escherichia coli* fadK (ydiD) gene encodes an anerobically regulated short chain acyl-CoA synthetase. J. Biol. Chem. *279*, 37324–37333.

Morsczeck, C., Berger, S., and Plum, G. (2001). The macrophage-induced gene (mig) of *Mycobacterium avium* encodes a medium-chain acyl-coenzyme A synthetase. Biochim. Biophys. Acta *1521*, 59–65.

Portevin, D., De Sousa-D'Auria, C., Houssin, C., Grimaldi, C., Chami, M., Daffe, M., and Guilhot, C. (2004). A polyketide synthase catalyzes the last condensation step of mycolic acid biosynthesis in *Mycobacteria* and related organisms. Proc. Natl. Acad. Sci. USA *101*, 314–319.

Portevin, D., de Sousa-D'Auria, C., Montrozier, H., Houssin, C., Stella, A., Laneelle, M.A., Bardou, F., Guilhot, C., and Daffe, M. (2005). The acyl-AMP ligase FadD32 and AccD4-containing acyl-CoA carboxylase are required for the synthesis of mycolic acids and essential for mycobacterial growth: identification of the carboxylation product and determination of the acyl-CoA carboxylase components. J. Biol. Chem. *280*, 8862–8874.

Post-Beittenmiller, D., Jaworski, J.G., and Ohlrogge, J.B. (1991). In vivo pools of free and acylated acyl carrier proteins in spinach. Evidence for sites of regulation of fatty acid biosynthesis. J. Biol. Chem. *266*, 1858–1865.

Reger, A.S., Carney, J.M., and Gulick, A.M. (2007). Biochemical and crystallographic analysis of substrate binding and conformational changes in acetyl-CoA synthetase. Biochemistry *46*, 6536–6546.

Reger, A.S., Wu, R., Dunaway-Mariano, D., and Gulick, A.M. (2008). Structural characterization of a 140 degrees domain movement in the two-step reaction catalyzed by 4-chlorobenzoate:CoA ligase. Biochemistry *47*, 8016–8025.

Rock, C.O., Cronan, J.E., Jr., and Armitage, I.M. (1981). Molecular properties of acyl carrier protein derivatives. J. Biol. Chem. *256*, 2669–2674.

Rusnak, F., Faraci, W.S., and Walsh, C.T. (1989). Subcloning, expression, and purification of the enterobactin biosynthetic enzyme 2,3-dihydroxybenzoate-AMP ligase: demonstration of enzyme-bound (2,3-dihydroxybenzoyl)adenylate product. Biochemistry *28*, 6827–6835.

 ©2009 Elsevier Ltd All rights reserved

Shanklin, J. (2000). Overexpression and purification of the *Escherichia coli* inner membrane enzyme acyl-acyl carrier protein synthase in an active form. Protein Expr. Purif. *18*, 355–360.

Shiraishi, T., Tezuka, K., and Uda, Y. (1994). Selective inhibition of lignoceroyl-CoA synthetase by adenosine 5′-alkylphosphates. FEBS Lett. *352*, 353–355.

Sieuwerts, A.M., Klijn, J.G., Peters, H.A., and Foekens, J.A. (1995). The MTT tetrazolium salt assay scrutinized: how to use this assay reliably to measure metabolic activity of cell cultures in vitro for the assessment of growth characteristics, IC50-values and cell survival. Eur. J. Clin. Chem. Clin. Biochem. *33*, 813–823.

Takayama, K., Wang, L., and David, H.L. (1972). Effect of isoniazid on the in vivo mycolic acid synthesis, cell growth, and viability of *Mycobacterium tuberculosis*. Antimicrob. Agents Chemother. *2*, 29–35.

Trivedi, O.A., Arora, P., Sridharan, V., Tickoo, R., Mohanty, D., and Gokhale, R.S. (2004). Enzymic activation and transfer of fatty acids as acyl-adenylates in mycobacteria. Nature *428*, 441–445.

Wong, H.C., Liu, G., Zhang, Y.M., Rock, C.O., and Zheng, J. (2002). The solution structure of acyl carrier protein from *Mycobacterium tuberculosis*. J. Biol. Chem. *277*, 15874–15880.

 ©2009 Elsevier Ltd All rights reserved

Chemistry & Biology *16*

Supplemental Data

The Dual Function of the

Mycobacterium tuberculosis FadD32

Required for Mycolic Acid Biosynthesis

Mathieu Léger, Sabine Gavalda, Valérie Guillet, Benoît van der Rest, Nawel Slama, Henri Montrozier, Lionel Mourey, Annaïk Quémard, Mamadou Daffé, and Hedia Marrakchi

SUPPLEMENTAL MATERIALS

The sources of [1-^{14}C]fatty acids (specific activity, 50-58 mCi/mmol) were the American Radiolabeled Chemicals, Inc. (St Louis, MO) and PerkinElmer (Waltham, MA). ACP, antibiotics and most other chemicals were purchased from Sigma (St Louis, MO), whereas microbiological media were ordered from Invitrogen (Carlsbad, CA) and Difco (by VGDINC, Lawrence, KA). Restriction enzymes were purchased from New England Biolabs (Ipswich, MA) and DNA purification kits from Qiagen (Courtaboeuf, France), whereas chromatography columns and FPLC system were from GE Healthcare (Piscataway, NJ). Acyl-AMP standards were synthesized according to (Keller et al., 1984). Proteins were quantitated by either the Bradford method (Bradford, 1976) using bovine serum albumin as a standard, or using the calculated extinction coefficient.

SUPPLEMENTAL EXPERIMENTAL PROCEDURES

Cloning and Purification of FadD32 (His$_6$-FadD32)

The *fadD32* gene was amplified from the bacterial artificial chromosome (BAC) library of *M. tuberculosis* H37Rv (Institut Pasteur). The *fadD32* PCR primer pair consisted of 5'-ACGTCATATGTTTGTGACAGGAGAGAG and 5'-ATGCAAGCTTGTCCGAAGTGGCGAAGACCG. The primers introduced the restriction sites for *Nde*I at the initiator methionine codon of the predicted coding sequence and *Hind*III downstream of the stop codon. The PCR products were ligated into the pGEM-T vector according to the manufacturer's instructions (Promega, Madison, WI) and the insert was confirmed by DNA sequencing with T7 and SP6 primers. The single *Nde*I digestion released the *fadD32* fragment from pGEM-T (having a *Nde*I site downstream of the cloned insert). The insert was then isolated and ligated into the pET15b *Escherichia coli* expression vector (Novagen) under the control of the *T7* promoter. Restriction profiles allowed the selection of the forward orientation of the insert in the resulting plasmid (pET15b-*fadD32*), that was used to transform the *E. coli* BL21(DE3) strain. The recombinant cells were grown at 37 °C in LB medium containing carbenicillin (50 µg ml^{-1}) and induced at OD_{600}= 0.5 by adding 0.5 mM isopropyl thio-β-D-galactopyranoside. Cells were then grown 5 h at 25°C and collected by centrifugation at 4,000 g for 15 min at 4°C, washed in [50 mM Tris pH 8, 500 mM NaCl, 10% glycerol] and kept at -80°C until further use. For lysis, pellets were resuspended (1:25 dilution of culture volume) in [50 mM Tris pH 8, 500 mM NaCl, 10% glycerol, 0.75 mg ml^{-1} lysozyme, 1 mM phenylmethylsulfonyl fluoride (PMSF)] supplemented or not with 30 mM imidazole and frozen overnight at -80°C. All further purification steps were performed at 4°C. The frozen bacterial pellets were thawed at room temperature and disrupted by sonication (5 intermittent pulses of 30 s in ice) on a VibraCell (Fisher Bioblock Scientific, Illkirch, France). Cell debris were removed by centrifugation (60 min

at 45,000 g) and the cleared lysate was filtered on 0.2 µm (Millipore) and applied to HisTrap™ HP (1 ml) affinity column. Elution of the protein from the affinity column (monitored at OD_{280}) was performed using two different gradients: "imidazole" or "pH". For the "imidazole" elution, the cleared lysate was loaded onto the column that was washed with 10%, then with 20% buffer B [50 mM Tris pH 8, 300 mM imidazole, 300 mM NaCl, 10% glycerol, 0.2 mM PMSF]. The His_6-tagged protein was eluted with 50% of buffer B. For the "pH" elution procedure, the affinity column was sequentially washed with buffers with decreasing pH, all containing 500 mM NaCl, 10% glycerol, 0.2 mM PMSF: buffer A1 [50 mM Tris, pH 8]; buffer A2 [20 mM NaH_2PO_4, pH 7.3]; buffer A3 [20 mM sodium acetate, pH 6] and 20% of buffer B3 [20 mM sodium acetate, pH 4] (in A3). The His_6-tagged protein was eluted with 60% of buffer B3. The combined fractions corresponding to the FadD32 peak were applied to a gel filtration chromatography (Superdex 200) column pre-equilibrated with [50 mM Tris pH 8, 500 mM NaCl, 0.2 mM PMSF]. The protein was homogeneous as judged by sodium dodecyl sulfate-polyacrylamide gel electrophoresis (Laemmli, 1970) and western blot analysis.

Western Blot Analysis of the His_6-FadD32

The western blot analysis of His_6-FadD32 from different purification stages was performed using standard protocols. Briefly, samples were separated on 12% SDS-PAGE (using a Mini-Protean II electrophoresis system, Bio-Rad) and the proteins were electrophoretically transferred to nitrocellulose membrane (Trans-blot SD semi-dry transfer cell, Bio-Rad). The membranes were pre-blocked in 5% nonfat milk powder and then incubated overnight with anti-poly histidine antibodies (Sigma) diluted 1:2000. The membranes were washed and incubated with secondary antibodies conjugated with alkaline phosphatase (Sigma, 1:10000); the labeled His-tagged proteins were visualized using BCIP/NBT Color Development Substrate kit (Promega) for the colorimetric detection of alkaline phosphatase activity.

Kinetic Parameter Determinations

For the determination of apparent kinetic parameters, the concentration of one substrate was varied in the presence of constant levels of the second substrate or cofactor. The substrate concentrations varied generally from 0.2 to 5-10 times the K_m value. The apparent K_m and k_{cat} values of the enzyme for the fatty acids were found similar at all concentrations examined of ATP (2 to 10 mM); for instance, K_m of 20.5 and 18.8 µM were obtained for the C14:0 with 2 and 10 mM ATP, respectively. However, the addition of concentrations of ATP higher than 5 mM in the assay (to approach saturating concentrations) resulted in a severe decrease in reaction rates, with V_{max} being significantly reduced (from 3.7 to 0.18 pmole/min in the presence of 2 and 10 mM ATP, respectively). Accordingly, the kinetic parameters determination of fatty acids was performed in the presence of 2 mM ATP.

Competition Studies

Because of the unavailability of commercially radiolabeled fatty acids longer than C20, the fatty acid substrate specificity of the purified FadD32 was assessed using a competitive enzymatic inhibition by the addition of unlabeled fatty acids. The competing long- and very long-chain fatty acids were added at a fixed concentration (10 µM) to the reaction containing increasing concentrations of [^{14}C]palmitic acid.

Chemical synthesis of the acyl-AMP analog (alkyl-AMP)

The adenosine 5'-alkylphosphate (AMPC12) was chemically synthesized from alkyl bromide and AMP tetrabutylammonium salt in dimethylacetamide at 80°C for 4 h, as described previously (Machida et al., 1997). The synthesized alkyl-AMP was purified by flash chromatography on a silica gel (Florisil) column. The chemical structure of the alkyl-AMP (AMPC12) was confirmed by mass spectrometry and NMR spectroscopy. The MALDI-TOF (Matrix Assisted Laser Desorption Ionisation - Time Of Flight) MS mass spectra were characterized by the occurrence of

the pseudo molecular ions ($M+H^+$), ($M+Na^+$) and ($M-H+2Na^+$) at *m/z* 516, 538 and 560, respectively. Analysis of the ^{1}H-NMR (600 MHz in DMSO-d6) spectra was in good agreement with the previously reported data for AMP analogs (Machida et al., 1997), namely, the characteristic signals for adenosine ring at 8.39 p.p.m (singlet, 1H) and 8.22 p.p.m (singlet, 1H); the signal resonances for ribofuranose were observed at 5.96 p.p.m (doublet, 1H, J = 4.3, H'1), 4.62 p.p.m (triplet, 1H, J = 5.2, H'2), 4,22 p.p.m. (triplet, 1H, J = 4.62, H'3), 4.11 p.p.m (multiplet, 1H, H'4), and 4.05 p.p.m (multiplet, 2H, H'5,5'), respectively. Signal resonances of CH_2 linked to phosphate group were seen at 3.84 p.p.m (multiplet, 2H, J_{CH2}, P = 6.7) and 1.53 p.p.m. (multiplet, 2H) and those for aliphatic chain were observed at 1.23 p.p.m (multiplet, CH_2) and 0.87 ppm (triplet, 3H, J = 7.1, CH_3).

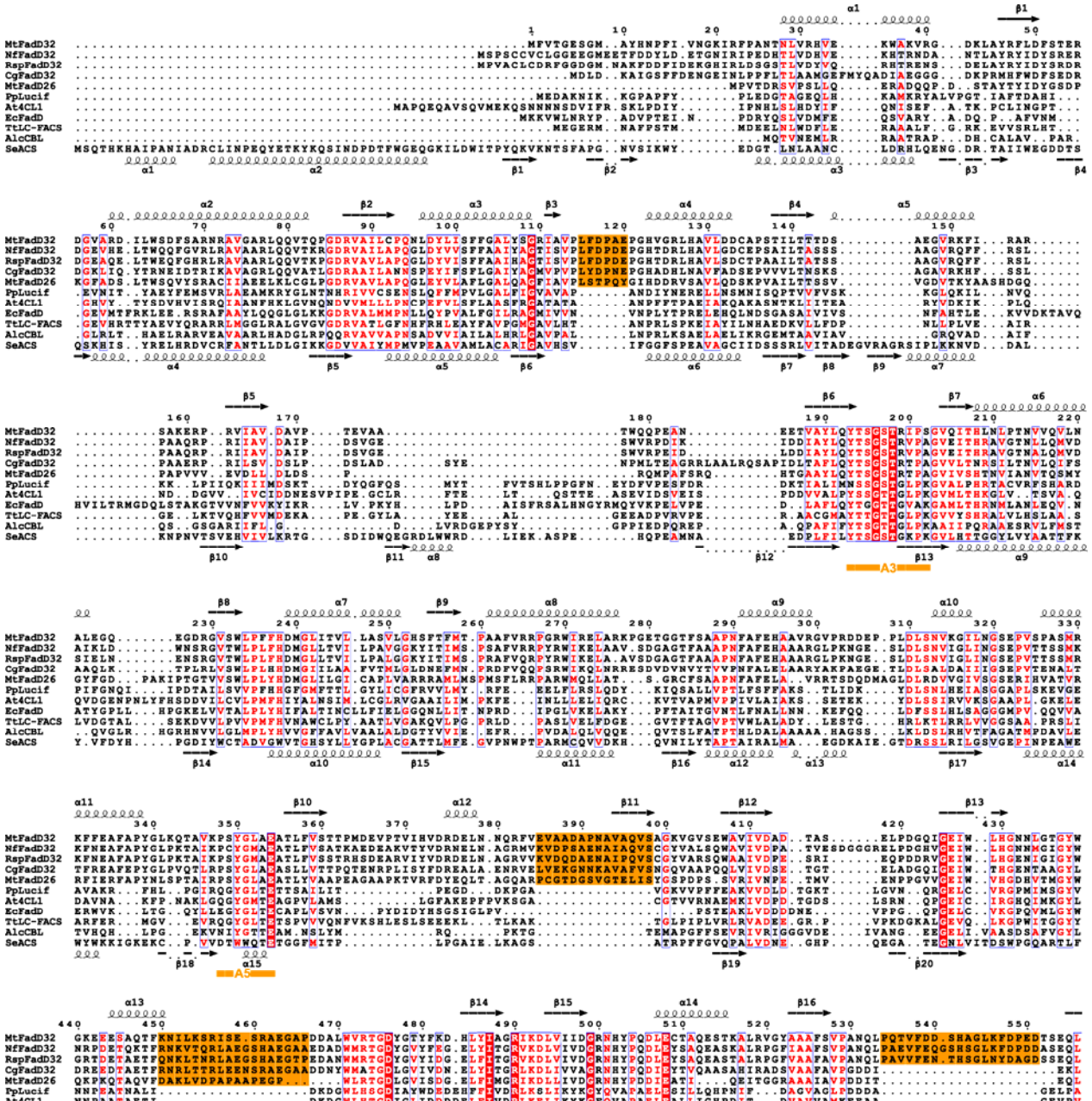

Figure S1. Structure-Based Amino Acid Sequence Alignment of FadD32 with Other Adenylate-Forming Proteins

Sequences of various members of the adenylate-forming protein superfamily were aligned using Clustal W2 (Larkin et al., 2007). MtFadD32 (*M.tuberculosis* FadD32, CAA17865); NfFadD32 (*Nocardia farcinica* FadD32, YP_116394); RspFadD32 (*Rhodococcus* jostii RHA FadD32, YP_704019); CgFadD32 (*Corynebacterium glutamicum* FadD32, CAF20897); MtFadD26 (*Mycobacterium tuberculosis* FadD26, Q10976) PpLucif (*Photinus pyralis* luciferase, BAF48396); At4CL1 (*Arabidopsis thaliana* 4-coumarate-CoA ligase, Q42524); EcFadD

(*Escherichia coli* FadD, CAA50321); TtLC-FACS (*Thermus thermophilus* long-chain fatty acyl-CoA synthetase, BAD20228); AlcCBL (*Alcaligenes sp.* chlorobenzoate-CoA ligase, AAN10109); SeACS (*Salmonella enterica ser tiphymurium* acetyl-CoA synthetase, AAO71645). The structural alignment was performed using DaliLite server for the available structures at the Protein Data Bank PDB (Holm and Park, 2000) and manual adjustment was done in Seaview (Galtier et al., 1996). Alignments were obtained using Espript (Gouet et al., 1999). Similarity scores higher than 60% are represented in red characters on a white background; white characters on a red background correspond to residues strictly conserved in the column. Secondary structure prediction was obtained for MtFadD32 sequence by NPS@ (Combet et al., 2000) and is represented at the top of the structural alignment. PpLucif (PDB 1BA3); TtLC-FACS (PDB 1ULT), AlcCBL (PDB 3CW8) and SeACS (PDB 1PG4) structures have been superimposed using DaliLite pairwise structural alignments. Secondary structure of the SeACS is represented at the bottom row. The highly conserved patches A3 to A10 within the conserved domains are indicated with solid lines below the sequences; the insertions within the FadD32 sequences are highlighted in yellow boxes.

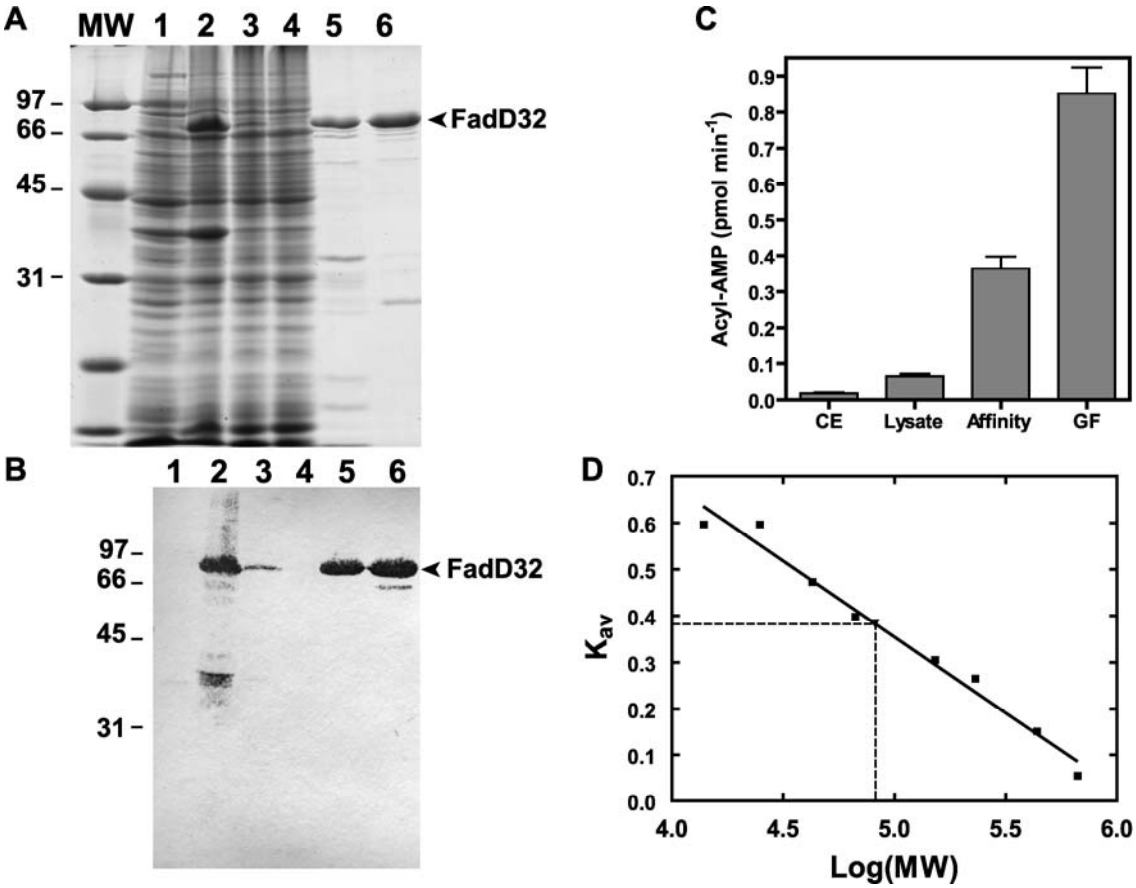

Figure S2.
(A) SDS-PAGE purification steps of His_6-FadD32. Recombinant FadD32 was expressed and purified and fractions were taken throughout the purification process and assayed for C14-AMP formation activity as described under “Experimental Procedures”. Lane 1, uninduced culture; lane 2, crude extract (CE); lane 3, soluble lysate fraction (lysate); lane 4, nickel affinity chromatography flow-through; lane 5, pool of fractions eluted from the nickel affinity column (at pH 5.3); lane 6, pool of fractions eluted from gel filtration S200 column (GF).
(B) Western blot analysis of FadD32-containing fractions during the purification process using anti-His antibodies.
(C) Fatty acyl AMP-ligase (FAAL) activity measured in the FadD32-containing fractions (CE, lysate, affinity, GF) obtained during the purification process. Two µg of total protein in each

fraction was assayed using [1-^{14}C]C14 as substrate; data are the mean of two replicates ± standard error of the mean (SEM).
(D) The apparent molecular mass of FadD32 was estimated by gel filtration chromatography using a Hi-load 16/60 Superdex 200 prep grade column (GE Healthcare) calibrated with RNase A (14 kDa), chymotrypsin (25 kDa), ovalbumin (43 kDa), albumin (67 kDa), aldolase (153 kDa), catalase (232 kDa), ferritin (440 kDa), and thyroglobuline (669 kDa). The column, pre-equilibrated with [50 mM Tris pH 8, 500 mM NaCl, 0.2 mM PMSF], was developed at a flow rate of 0.5 mL/min and the elution volumes of standards allowed calculation of K_{av} (V_e-V_0/V_t-V_0), where V_e, V_0 and V_t represent the elution volume, the column void volume and the column total volume, respectively.

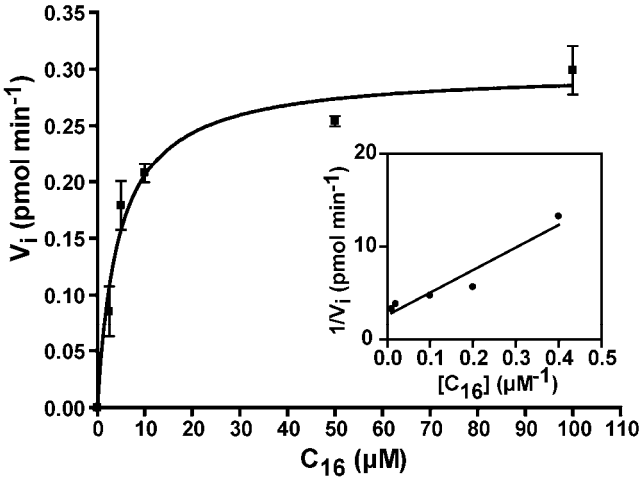

Figure S3. FadD32-Catalyzed Reaction Rate
Formation of acyl-AMP by FadD32 (2 µM) was followed as a function of [1-^{14}C]C16 concentration in a typical radio-TLC assay and quantified by phosphorimager. Data show means of triplicate reactions ± SEM. *Inset*, Lineweaver-Burk plot of the enzyme reaction.

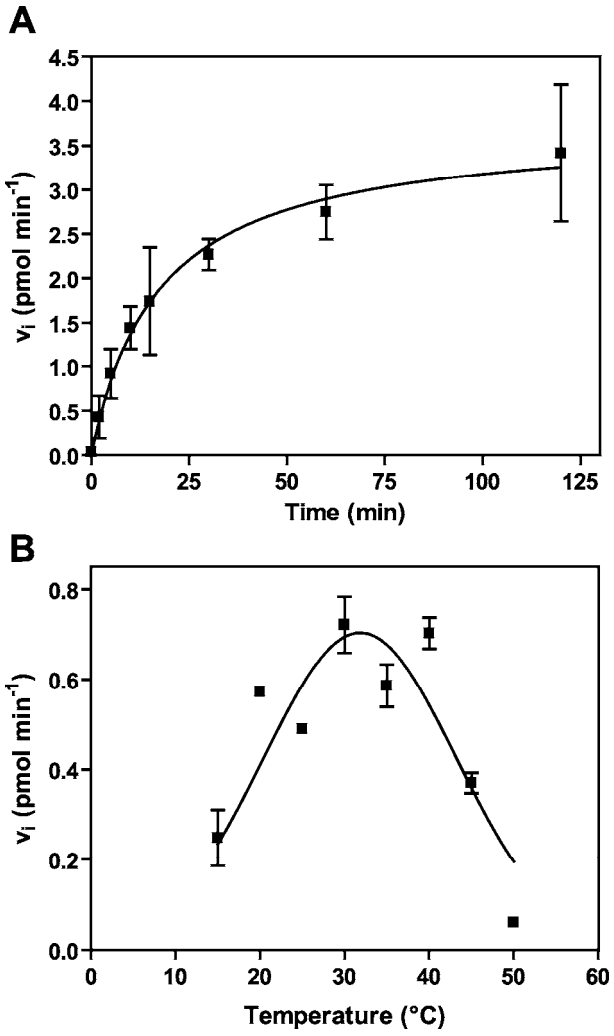

Figure S4. Determination of Optimal Assay Conditions for FadD32 Activity
FadD32 was purified using affinity chromatography (imidazole gradient) followed by gel filtration chromatography as described under "Experimental procedures". Experiments for time course (A) and determination of the temperature effect on the FadD32 acyl-AMP activity (B) were performed using 2 µM FadD32 in the presence of 100 µM [1-^{14}C]C12:0; data are the mean of two replicates ± SEM.

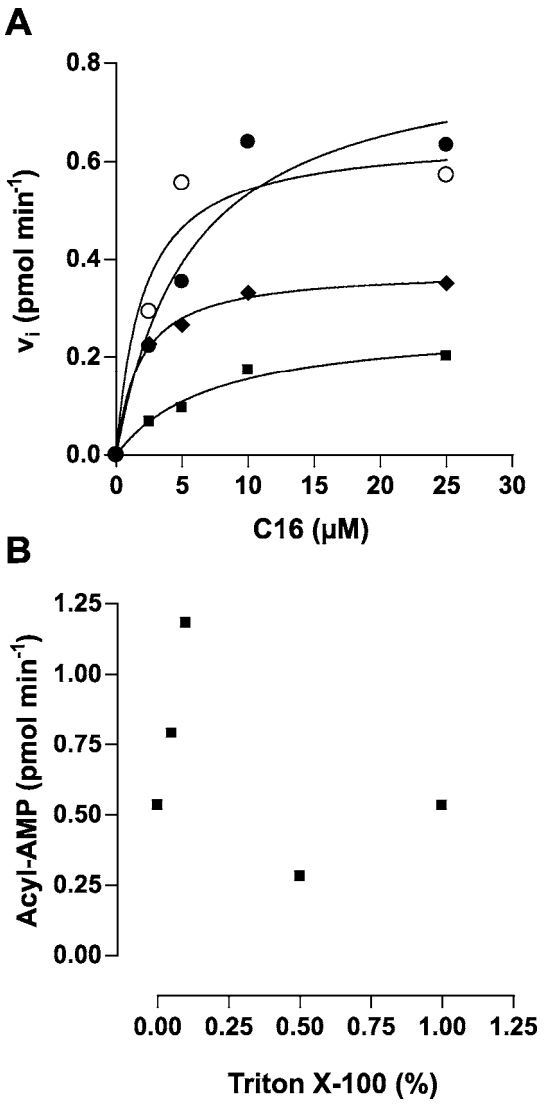

Figure S5.
(A) Competitive kinetic assay of FadD32 with very long-chain substrates. The acyl-AMP ligase activity of FadD32 (2 μM) was assayed using increasing concentrations of [1-^{14}C]C16 as substrate, in the absence (◆) or presence of 10 μM of the indicated cold fatty acids: C16:0 (■), C20:0 (○) or C24:0 (●).
(B) FadD32 activity in the presence of increasing concentrations of Triton X-100. The assay for FadD32 FAAL activity included 2 μM of the protein and 100 μM [1-^{14}C]C14:0 as the substrate, in the presence of the indicated concentrations (%, v/v) of Triton X-100.

SUPPLEMENTAL REFERENCES

Bradford, M. M. (1976). A rapid and sensitive method for the quantitation of microgram quantities of protein utilizing the principle of protein-dye binding. Anal. Biochem. 72, 248-254.

Combet, C., Blanchet, C., Geourjon, C., and Deleage, G. (2000). NPS@: network protein sequence analysis. Trends Biochem Sci 25, 147-150.

Galtier, N., Gouy, M., and Gautier, C. (1996). SEAVIEW and PHYLO_WIN: two graphic tools for sequence alignment and molecular phylogeny. Comput Appl Biosci 12, 543-548.

Gouet, P., Courcelle, E., Stuart, D. I., and Metoz, F. (1999). ESPript: analysis of multiple sequence alignments in PostScript. Bioinformatics 15, 305-308.

Holm, L., and Park, J. (2000). DaliLite workbench for protein structure comparison. Bioinformatics 16, 566-567.

Keller, U., Kleinkauf, H., and Zocher, R. (1984). 4-Methyl-3-hydroxyanthranilic acid activating enzyme from actinomycin-producing Streptomyces chrysomallus. Biochemistry 23, 1479-1484.

Laemmli, U. K. (1970). Cleavage of structural proteins during the assembly of the head of bacteriophage T4. Nature 227, 680-685.

Larkin, M. A., Blackshields, G., Brown, N. P., Chenna, R., McGettigan, P. A., McWilliam, H., Valentin, F., Wallace, I. M., Wilm, A., Lopez, R., Thompson, J. D., Gibson, T. J., and Higgins, D. G. (2007). Clustal W and Clustal X version 2.0. Bioinformatics 23, 2947-2948.

Machida, K., Tanaka, T., Shibata, K., and Taniguchi, M. (1997). Inhibitory effects of nucleoside 5'-alkylphosphates on sexual agglutination in Saccharomyces cerevisiae. FEMS Microbiol Lett 147, 17-22.

Table S1. Kinetic Parameters of FadD32 for Fatty Acid Substrates and ATP

	K_m (μM)	V_{max} (pmol min^{-1})	k_{cat} (min^{-1})	k_{cat}/K_m (mM^{-1} min^{-1})
C12[a]	2640	4.4	0.150	0.06
C14	20.5	3.7	0.123	6.0
C16	3.2	0.45	0.015	4.7
ATP	2020	1.25	0.09	0.04

FadD32 fatty acyl-AMP ligase activity was tested using the radio-TLC assay. Data of FadD32 kinetic constants were measured from initial velocity experiments and are representative of at least two independent experiments, each performed in 1-, 2- or 3- replicates. The steady-state parameters K_m (Michaelis constant), V_{max} (maximum velocity), k_{cat} (catalytic constant) and k_{cat}/K_m (catalytic efficacy) were determined using non-linear regression to fit the data to the Michaelis-Menten equation using the PRISM software (GraphPad Software Inc.). [a] Kinetic constant values measured for the C12 fatty acid displayed significant variations, yet the ratio k_{cat}/K_m remained in the same order of magnitude.

Table S2. Proximity of *fadD* Genes and (*acyl-/peptidyl-carrier protein*) *acp/pcp*-Coding Sequences in *M. tuberculosis* H37Rv Genome

fadD	**Neighboring *pks*, NRPS genes or *acp/pcp***		
	name	**adjacent**	**same orientation**
fadD21	-		
fadD23	*Rv3825c (pks2)*	-	-
fadD24	*pks5*	-	-
fadD25	-		
fadD26	*Rv2931 (ppsA)*	+	+
fadD28	*mas*	+	-
fadD29	*pks15, pks1*	-	+
fadD30	*Rv0405 (pks6)*	+	+
fadD31	-		
fadD32	*pks13*	+	+
fadD33	*Rv1344*	+	+
fadD34	*acpA*	+	+